Wind effects in the parametrisation of physical characteristics for a nearshore wave model

Lavidas, George; Polinder, Henk

Publication date
2019

Document Version
Final published version

Published in
Proceedings of the 13th European Wave Energy and Tidal Conference (EWTEC 2019)

Citation (APA)
Lavidas, G., & Polinder, H. (2019). Wind effects in the parametrisation of physical characteristics for a nearshore wave model. In *Proceedings of the 13th European Wave Energy and Tidal Conference (EWTEC 2019)* Article 1225 EWTEC.

13th ewtec 2019
Proceedings of the 13th European Wave and Tidal Energy Conference 1-6 Sept 2019, Naples, Italy

Wind effects in the parametrisation of physical characteristics for a nearshore wave model

George Lavidas and Henk Polinder

***Abstract*—To properly assess the energy and waves at a region, it is vital to obtain suitable long term metocean conditions. Although, wave buoys are a significant source of information they are not able to provide a detailed and complete resource assessment, as they have inherent spatio-temporal and recording limitations. Therefore, numerical wave models are often used to estimate wave power and metocean conditions. A wave model can provide realistic representation of physical processes, but it should entail careful tuning of parameters, which are often based on empirical and semi-empirical configurations.**

The study presents calibration of a wave numerical model and examines its performance, for nearshore wave assessments. Parametrisations of wind growth and white-capping coefficients have direct effects on evolution of locally generated waves, swells, and can reduce uncertainty in the results of a hindcast. The results are used to explain the physical meaning of differences, and provide a detail comparison of metocean parameters with nearshore and shallow water buoys as in-situ benchmarkers. Inter-model comparisons also indicate differences in spatial wave generation and propagation, as affected by wind growth and dissipation rates. The "optimal" solution will result in a model that will be used to provide a long-term high resolution metocean and wave power assessment for the Netherlands, that so far has been lacking in wave energy resource characterisation.

***Index Terms*—Wave modelling, Resource assessment, Whitecapps, Wind drag**

I. Introduction

WAVE assessments are vital tools for the viability and operational safety of any offshore activity. With focus on wave energy, resource quantification can provide valuable information on propagation, energy density, expected production, estimation of extreme events, variation, spatial distribution, and help us reduce uncertainties when it comes to long-term energy extrapolations.

Describing the wave climate is not straightforward, metocean conditions vary significantly pending on region, location, coastal depths, and surrounding topography. There are several ways to record and evaluate the wave resource, including but not limited to buoys, satellite, numerical wave models. Each methodology has its own positive and negative attributes, which should be considered.

Submission ID: 1225 WRC. G. Lavidas receives funding for the project WAve Resource for Electrical Production (WAVREP) by the European Union's Horizon 2020 research and innovation programme, under the Marie Skłodowska-Curie Individual Fellowship (MSCA-IF) grant agreement No 787344.

G. Lavidas, Mechanical, Maritime and Materials Engineering (3mE), Delft University of Technology (TU Delft), Mekelweg 2, 2628 CD Delft, The Netherlands (e-mail: G.Lavidas@tudelft.nl)

H. Polinder, Mechanical, Maritime and Materials Engineering (3mE), Delft University of Technology (TU Delft), Mekelweg 2, 2628 CD Delft, The Netherlands (e-mail: H.Polinder@tudelft.nl)

A resource assessment needs to cover a wide range of spatial and temporal condition, providing metocean data that can accurately be used for an energy study. While, satellites have evolved significantly, they have several spatio-temporal limitations which hinder their applicability for wave energy resource assessments [1]–[3]. Buoys and other point location mechanisms can have long-term conditions recorded, but their spatial applicability is limited. Numerical wave model are "powerful" tools that, if properly used can provide detail evaluation of the wave resource, and reduce assumption of wave energy applications [4], [5].

However, numerical wave models are not easy to use and depend on the experience and set-up by the user. Evolution f our knowledge in wave theory has resulted in the development of empirical and semi-empirical coefficients, to describe phenomena in wave generation, propagation and dissipation. In addition, there are different models that use different numerical approaches to assess the wave resource [6].

This study focuses on the effects of wind schemes and whitecapping in the nearshore spectral wave model Simulating WAves Nearshore (SWAN) [7]. The calibration is conducted to ensure that an "optimal" configuration is developed to generate a wave energy and metocean resource database for the Netherlands, that will extend from the past and will be constantly updated forwards with time.

In order to do this, first a "reliable" model configuration must be developed. To date the Dutch coastlines do not have a study of this magnitude, scale and interest developed. Developing a wave energy database is imperative as the Dutch government is showing interest in this emerging from of ocean energy, but no detail spatial analysis exists to support evidence based development [6]. Model focus will be the development for offshore energies, therefore we consider that wave height agreement with historical in-situ measurements must be at least 90%. For the development of wave energy in the region it is vital to enhance knowledge in the potential and identify regions that can serve as fertile first generation areas.

The manuscript presents and discusses the calibration process for different wind schemes, different calibrated wind drag and whitecapping coefficients. The methodology describes differences per solution and discusses the performance of annual hindcast with in-situ (buoy) measurements. In addition, a comparative statistical analysis between all models is made, to determine the best solution for the reason of developing a wave energy resource database.

II. Materials & Methods

SWAN is a third generation spectral phased-averaged wave model, accounts multiple physical processes suitable for deep and shallow waters, although arguably it is more efficient for nearshore and Shelf Seas. The wave spectrum is described in time (t) by the action density equation (E), dependent upon angular frequency (σ), direction, frequency (f), energy propagation (c) over latitude (λ) and longitude (θ). Sink source terms are used to estimate the wave parameters (see Eq. 1), given a specific set of inputs and physical coefficients, with wind input (S_{in}), triads (S_{nl3}), quadruplet (S_{nl4}) interactions, whitecapping ($S_{ds,w}$), bottom friction ($S_{ds,b}$) and ($S_{ds,br}$) depth breaking.

$$S_{tot} = S_{in} + S_{nl3} + S_{nl4} + S_{ds,w} + S_{ds,b} + S_{ds,br} \quad (1)$$

In wave models generation, propagation and evolution of the wave spectrum is dependent on various parameters. Most important source terms are wind generation S_{in}, and dissipation $S_{ds,w/b/br}$ as they are the mechanisms responsible for wave generation and dissipation.

Wave are created by ocean wind surface pressure, in wave models this term is modelled by considering a wind drag coefficient that contributes to the growth. Wind wave generation is a summation of energy density $E(\lambda, \theta)$ (over Spherical coordinates), A is the linear growth and β exponential growth coefficient, respectively (see Eq: 2). Wind drag coefficients can differ and may enhance or reduce the wave generation capabilities in the model.

$$S_{in} = A + \beta E(\lambda, \theta) \quad (2)$$

In terms of dissipation mechanisms, most "obscure" and least understood is the white-capping $S_{ds,w}$ that is predominately based on a wave steepness coefficient (Γ), depending on a term adjustable and quite different for each methodology. It is known that wave models tend to under-estimate at lower frequencies, with accuracy also affected by wind components used. As a wind driver the ERA-Interim dataset form European Centre for Medium-Range Weather Forecasts (ECMWF) are used, with spatial resolution 0.125^o and time intervals 6 hours [8].

Other studies have used higher temporal wind datasets as drivers, that improved the "peak" wave performance (maxima values) but increased the scattering and significantly over-estimated higher frequencies [3], [9]. Given the fact that our interest is to generate a reliable wave energy and metocean database, main focus is to reduce the scattering and maintain close agreement with higher wave values, without over-predicting, as this can lead to over-estimating return values [10], and subsequently can lead to higher capital expenditure for infrastructure works. Similar, behaviour between different datasets has been also reported in other studies, with ERA-Interim exhibiting good performance with reduced scattering [11].

When utilising coarser resolution winds, or wind domains are comparatively larger than the domain resolution it is advised to perform parametric adaptation of key terms. This is a consideration that has to be taken, since the model that is used in this study, interpolates wind components over the domain used, that can lead to reductions in the generation of waves. There have been studies that used specifically produced domains with nested wind fields and increasing resolution [12].

While, this can lead to good results it also requires higher number of computational resource and calibration of the wind numerical model, ensuring its good performance. In this study the selection was done due to the fact that this re-analysis is based on Regional Climate Models adapted and the wind speeds exhibit better performance with measured data for the European continent. In addition, their open-source format ensures that our approach is re-producible.

For boundary conditions spectral information extracted by the WAve Model (WAM) from ECMWF, are applied throughout the open boundaries of the domain [13]. Bathymetry for the model is constructed on Spherical coordinates and utilizes ETOPO depth data and coastline information by the Global Self-consistent, Hierarchical, High-resolution Geography Database (GSHHG) [14]. The final domain is using an interpolation method and the resulted resolution corresponds to $\approx 0.025^o$ over (λ, θ), see Fig 1.

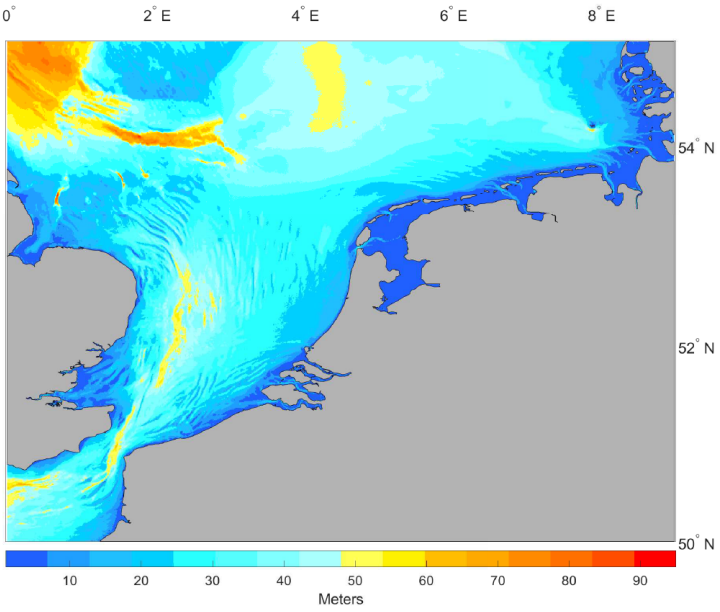

Fig. 1. Domain of calibration and depth in meters

III. Calibration

Recently SWAN 41.20 introduced an adjusted formulation for wind and whitecapping, similar but not exactly the same to WavewatchIII (WWIII) ST6 [15]. The wind drag parametrisation requires a finer tuning in the whitecapping coefficient. Interestingly for this new addition the solutions both for wind drag formulation and stress re-computation, allows for bias wind corrections, in the case that wind data are known to be under-estimated. In addition, the new formulation allows to include swell dissipation mechanisms.

An exponential growth coefficient is assigned for all configuration, and all models have a "hot" start

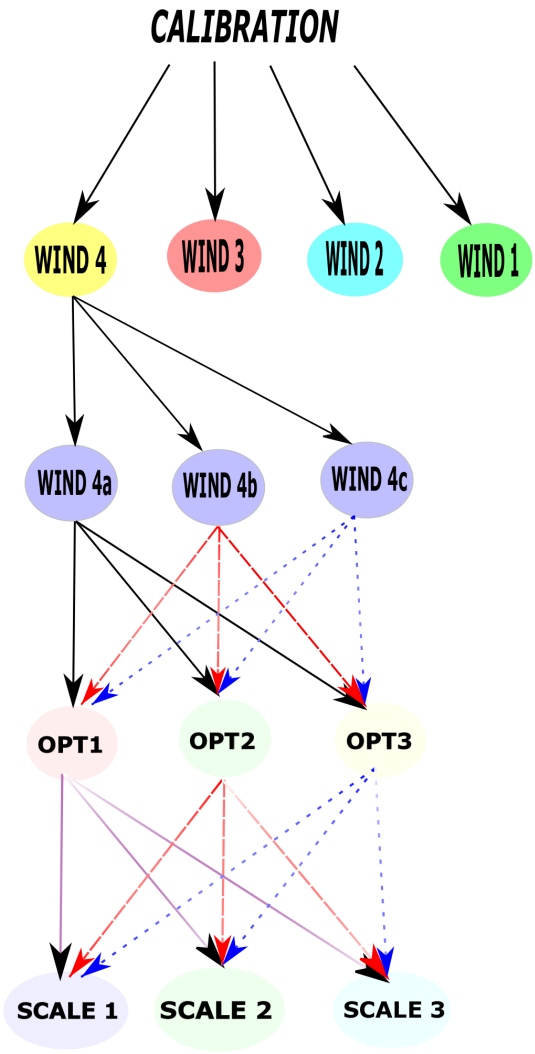

Fig. 2. Configuration for the calibration phase

configuration that ensures a fully developed wave field. Wind drag formulations are adjusted for every of the major wind schemes.

For wind 1 the configuration seen in Komen et.al [16] is set-up, where the wind drag coefficient (C_D) is dependent on the fiction velocity of wind speed (U_{10}) with adjustment $U_{10} < 7.5m/s$ and $U_{10} \geq 7.5m/s$.

For wind 2 the adjustments in proposed by Janssen [17], where the critical height is iteratively estimated according to its non-dimensional value.

For wind 3 option drag is based on the alternative description of van der Westhuysen et.al. [18].

Wind 4 represents the newly added ST6 package, and evaluates a different parametrisation both in wind drag, wind stress and whitecaps [19]. This newly imported package is similar to WWII but is implemented differently. The package includes swell dissipation influence in the estimations. In wind 4a the drag coefficient is adjusted according to Hwang et.al. [20], for wind 4b according to Fan et.al. [21], and wind4c is based on Janssen [17]. Within all different wind configuration the stress calculation is iteratively vectorally estimated, to enhance the wind drag.

For whitecapping, wind 1 and 4 use the WAM3 cycle, but a noticeable difference of the ST6 package, from WW3 and the other SWAN options for whitecaps is the use of a swell steepness dependent dissipation coefficient, is set at 1.2 according to Ardhuin et.al. [22]. Wind 2 uses the WAM4 cycle formulation. Bottom friction has been adjusted according to Zijlema et.al. [23] 0.038 m^2s^{-3}, nearshore breaking, triad interactions, and diffraction are all enabled based on their respective suggested values in SWAN. Quadruplets interactions for deeper water are resolved with a fully explicit computation per sweep, which makes the computation a bit more "expensive" but retains good agreement.

In the ST6 dissipation is described by local and cumulative terms, that cab be accordingly scaled, based on previous works on derivation of these terms the following "pairs" are utilised for dissipation (whitecapping effects) [7], [19], [24]. Option 1 has local dissipation (lds): 5.7^{-7} cumulative dissipation (cds): 8^{-6}, option 2 lds: 4.7^{-7}, cds: 6.6^{-6}, and option 3 lds: 2.8^{-6}, cds: 3.5^{-5}.

The scaling option parametrisation aims to correct the mean square slope, in this new term the suggestion is that the scale is over 28. Therefore, seeking to ensure a potential noticeable improvement we opted for three different tuning parameters, scale 1: 28, scale 2: 32 and scale 3: 35. Whilst more scaling can be attempted it is expected that the difference from 28 to 35 will be adequate to display any impacts on the hindcast. Tuning this option has to do with the amount of energy (more or less) that is allowed to migrate in higher frequencies. When the value is higher the amounts that are allowed there are reduced, therefore this can be beneficial to not under-estimate lower frequencies.

The explanatory naming sequence of the models is primarily based on Wind configuration, more specifically for the ST6 (wind 4) package the naming is *ST Wind4 x Opt x Scale x*, resulting in a numeric name for the model i.e. STE121 meaning a model that utilises the ECMWF wind configuration, with option 2 (for local & cumulative dissipation) and Scale 1, see Fig 2. All the calibration models were tuned using binned distribution of 36 directions and frequencies, with the latter using a Δf=0.1. The calibrations were conducted with an Intel Xeon with 36 GB of RAM.

IV. Results

To assess model results several indices are used, Pierson's correlation coefficient (R) indicates how well the hindcast performed (see Eq. 3), the root-mean-square-error ($RMSE$) underlines the differences between hindcast and buoy measurements (see Eq. 4), the Scatter Index (SI) give us an indication on the relationship between observed and modelled data (see Eq. 5). The goal of a good hindcast is to obtain high values of significant wave height (H_{m0}) $R \geq 85 - 90\%$, with $RMSE$ showing a close "positioning" with the mean values, a low $SI \leq 25 - 30\%$ (or high inverse $SI_{inv} \geq 85 - 90\%$). From experience we are aware under-estimation in wave models, therefore, we also compare the maximum values of significant wave height (H_{max}), to ensure that not only the mean bias is

TABLE I
BUOY INFORMATION

In-Situ	Longitude	Latitude	
In-Situ (Buoy)	Longitude	Latitude	Map Number
Brouwershavensegat	3,61^o	51,76^o	1
Schouwenbank	3,31^o	51,74^o	2
Eurogeul DWE	3^o	51,94^o	3
Europlatform 3	3,27^o	51,99^o	4
IJgeulstroompaal 1	4,51^o	52,46^o	5
IJmuiden Munitiestort 2	4,05^o	52,55^o	6
L91	4,96^o	53,61^o	7
F161	4,01^o	54,11^o	8
J61	2,95^o	53,81^o	9
F3 platform	4,72^o	54,85^o	10

low (see Eq. 6), but the bias of maxima events is also reduced by the model. This is considered helpful as it will translate to improvements in estimating statistically extreme return wave periods, and making the final model more versatile.

$$R = \frac{\sum_{i=1}^{N}((M_i - \overline{M_i})(O_i - \overline{O_i}))}{\sqrt{((\sum_{i=1}^{N}((M_i - \overline{M_i})^2)((\sum_{i=1}^{N}((O_i - \overline{O_i})^2)}} \quad (3)$$

$$RMSE = (\frac{1}{N}\sum_{i=1}^{N}(M_i - O_i)^2)^{0.5} \quad (4)$$

$$SI = \frac{RMSE}{\frac{1}{N}\sum_{i=1}^{N} O_i} \quad (5)$$

$$BIAS = \sum_{i=1}^{N}\frac{1}{N}(M_i - O_i) \quad (6)$$

where M_i is the simulated wave parameter, O_i recorded and N measurements.

Primary focus of the calibration is to ensure a good generation of past wave events in order to develop the wave power database. To examine the calibration of our models wave data from buoy measurements in 2015 were gathered [25], filtered by removing non-operational days, see Table I and Fig 3.

In total 30 calibration model performance was assessed by taking into account aforementioned indices and runtime. From experience we are aware than using the ERA-Interim dataset will reduce the maxima performance, if no calibration of the whitecapping coefficient is made, so as a final qualitative metric we also examined the ability of modelled data being close to maximum wave height values. Ideally, the bias will be near zero, and the maximum values will be closely followed, as they are important for extreme value analysis, moorings and structural estimations. If only interested in obtaining higher maxima values we would have opted using Climate Forecast System Reanalysis (CFSR) data which have shown a better maximum peak performance, however with means over-estimations and larger scattering in the North Sea [3].

In Fig. 4 the histograms of significant wave height (H_{m0}) for all calibration models are given, each model

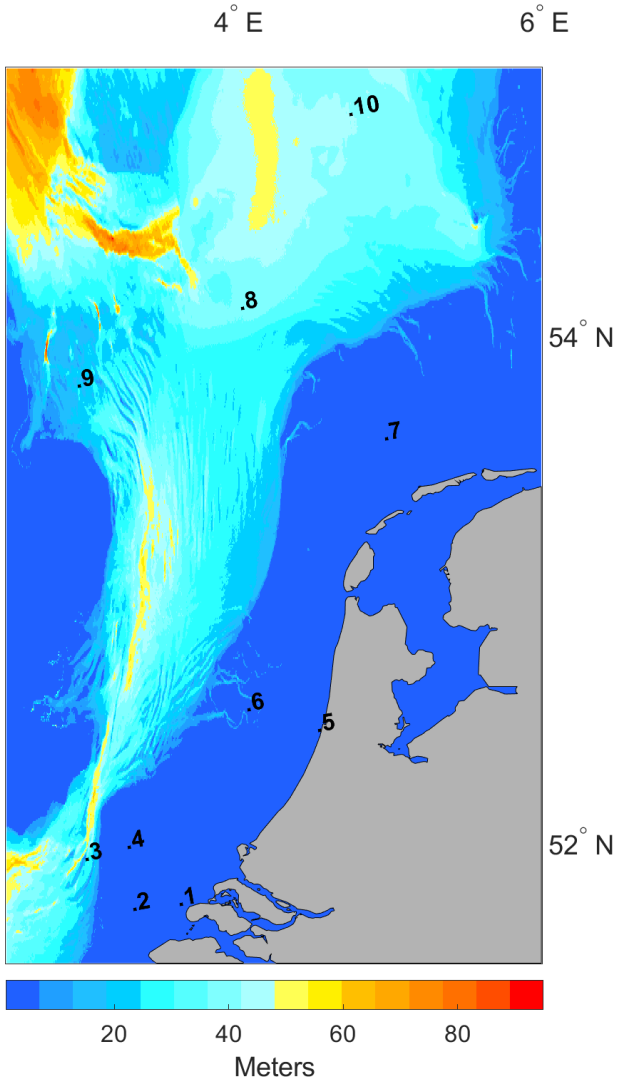

Fig. 3. In-situ instruments deployment depths

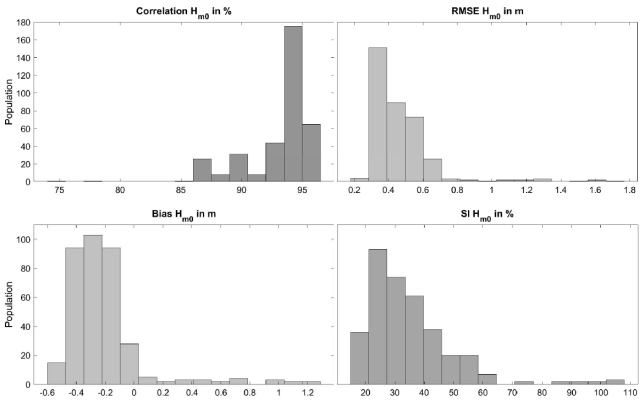

Fig. 4. Histograms of H_{m0} indices for all calibration models, values at the y-axis is common for all plots.

produced maps and 10 locations that correspond to buoys were extracted to assess the performance, comparing with real data. In total 300 points for were compared with in-situ measurements and the most suitable model was selected. For H_{m0} most locations showed a high correlation coefficient from 93-97%, the mean bias clustered at small under-estimations for H_{m0}

with $\approx$ 300 compared locations having a very small difference from -0.5 to 0.1 m, the RMSE is also limited with most compared data from 0.3 to 0.6 m. Finally, scattering of the results is within 18-25%, showing a strong agreement, see Table II.

TABLE II
AGGREGATE PERFORMANCE OF H_{m0} FOR ALL LOCATIONS

H_{m0}	R	RMSE (m)	Bias (m)	SI
Brouwershavensegat	90%	0,36	-0,17	37%
Europlatform 3	94%	0,46	-0,24	35%
Eurogeul DWE	94%	0,46	-0,23	34%
F3 platform	94%	0,53	-0,17	28%
F161	95%	0,50	-0,14	29%
Ijgeulstroompaal 1	94%	0,50	-0,32	41%
Ijmuiden Munitiestort 2	94%	0,45	-0,24	35%
J61	34%	0,47	-0,18	32%
L91	96%	0,42	-0,10	28%
Schouwenbank	93%	0,43	-0,21	35%

TABLE III
AGGREGATE PERFORMANCE OF T_{m02} FOR ALL LOCATIONS

T_{m02}	R	RMSE	Bias (sec)	SI
Brouwershavensegat	76%	1,15	-0,90	28%
Europlatform 3	82%	1,30	-1,16	28%
Eurogeul DWE	82%	1,19	-1,04	28%
F3 platform	78%	1,07	-0,68	20%
F161	78%	1,26	-0,99	24%
Ijgeulstroompaal 1	81%	1,11	-0,88	25%
Ijmuiden Munitiestort 2	81%	1,19	-1,01	26%
J61	79%	1,07	-0,78	22%
L91	82%	1,44	-1,20	27%
Schouwenbank	79%	1,24	-1,09	28%

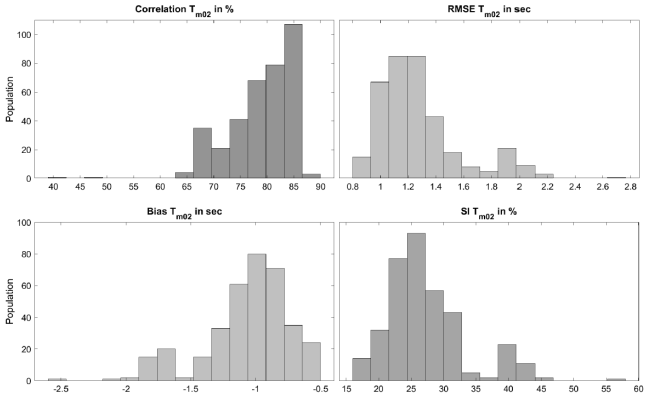

Fig. 5. Histograms of T_{m02} indices for all calibration models, values at the y-axis is common for all plots.

Performance of the zero crossing period (T_{m02}) was also assessed, these comparisons obtained lowered correlations when compared with the H_{m0}, but are in line with the numerical wave model performance for hindcasting period as they tend to have smaller correlations, Fig. 4. For T_{m02} the R shows that most skilled models are within the range of 80-90%, the RMSE is quite low from 0.5-1.5 seconds. This leads to a very small bias with most results showing small underestimations in line with the performance for H_{m0} mean bias. Finally, the calibration mean biases are located in the density of 20-27%, see Table III.

The histograms displayed that all configuration are able to hindcast the wave quantities in close agreement, however only one model configuration can be selected for the hindcast. Most models offer good correlations and almost all have a minimal bias with underestimations. Fig 6 shows R and inverse SI with regards to H_{m0} for all the models at platform F3 ($4,72$ East, $54,85$ North). Following the trend of the histograms most models have a good R, the highest one is given by the K_1 with 96% and SI 20% (inverse 80%). However, when also accounting the other indices STH_{113}, STH_{123}, STH_{133} have better performance with lower SI (19%), a significant low bias -0.04 m, while K_1 bias is -0.18, the RMSE is also smaller with 0.35 for the STH "family" and 0.37 m for K_1.

Noticeable all ST6 "families" that share the same wind drag and scale coefficients, have almost identical performance. Indicatively for the F3 location there are differences based on the rate of dissipation, but these predominately affect biases and maxima as shown in Table IV and Fig. 6 for F3.

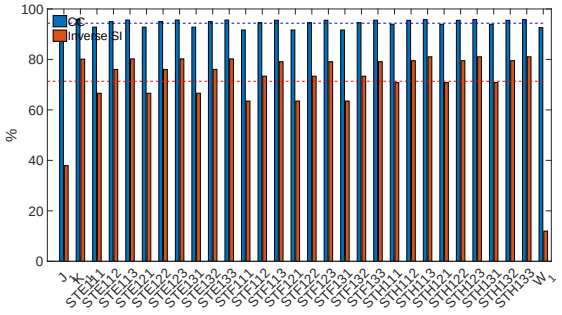

Fig. 6. Comparison of calibrating models

TABLE IV
PLATFORM F3 CALIBRATION RESULTS H_{m0}

H_{m0}	STH_{111}	STH_{112}	STH_{113}
R	93,95%	95,51%	95,77%
RMSE	0,54	0,38	0,35
Bias (m)	-0,37	-0,18	-0,04
SI	29,19%	20,50%	18,96%
Maxima (m)	6.31	7.03	7.56
Hours	27.66	27.85	27.99
	STH_{121}	STH_{122}	STH_{123}
R	93,95%	95,51%	95,77%
RMSE	0,54	0,38	0,35
Bias (m)	-0,37	-0,18	-0,04
SI	29,19%	20,50%	18,96%
Maxima (m)	6.31	7.03	7.56
Hours	27.56	27.77	27.90
	STH_{131}	STH_{132}	STH_{133}
R	93,95%	95,51%	95,77%
RMSE	0,54	0,38	0,35
Bias (m)	-0,37	-0,18	-0,04
SI	29,19%	20,50%	18,96%
Maxima (m)	6.31	7.03	7.56
Hours	27.65	27.77	27.99

With such small differences in ST6 calibrations, the maximum value of H_{m0} was also used as a metric of merit. For F3 the recorded maximum H_{max} is 7.98 m, therefore we also consider that the calibrated model should also be able to overcome the often under-performance in maxima. The calibration models with the first wind drag and third scaling coefficient achieved the highest maxima, therefore these seem to be the most "accurate" configuration, see Figs. 7-8. Since the indices have little to no difference, the

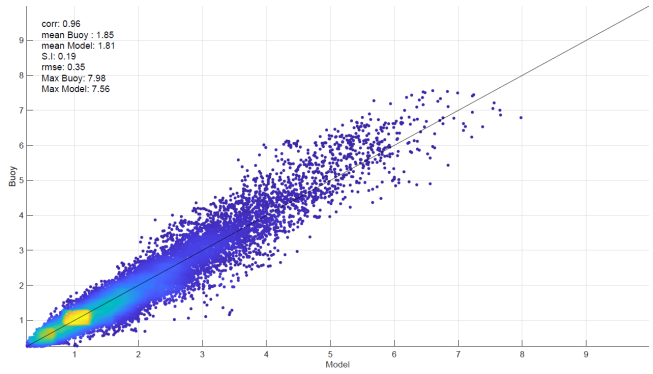

Fig. 7. H_{m0} of the "good model" based on ST6 parametrisation

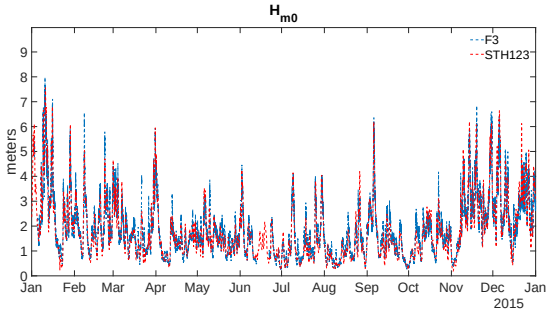

Fig. 8. Comparison of in-situ data with "good" configuration

hours run time to complete the hindcast was also assessed. The hindcast configuration has to be the one with highest correlation, closest maximum, lowest biases, RMSE, SI but at the same time must also be computational economical. As it can be seen from Fig. 8, the generation trend is closely followed and the maxima of recorded waves are also well captured. Assessment of all buoy location was conducted for all configurations and out of the 30 calibration models STH_{123} was found to be better 27 times, followed 3 times for K_1 (comparison with 300 resulted points 12 locations per calibration).

For all configuration the mean H_{m0} was estimated, similar to Fig. 9 but displaying the spatial distribution across the domain, with higher waves are encountered at Northern parts. When compared with K_1 the STH_{123} exhibits 10 cm difference in H_{m0} at nearshore regions and 15 cm at deeper water (see Fig. 10), indicating that there would be significant under-estimation of the propagating wave fields and subsequently of potential energy flux. The spatial differences between Hwang calibration models is very small in the effect of $\approx \pm 2^{-6}$, when also compared with the other wind configuration then majority of differences is found at deep and nearshore areas, when the "optimal" configuration is assessed with the similar option and scale but different wind drag STE_{123}, the highest difference is $\approx$ 12 cm at deep waters, and $1-2$ cm along the coastlines. When compared with STF_{123}, there is a higher difference $\approx$ 18 cm and $3-4$ cm for deeper and nearshore regions respectively.

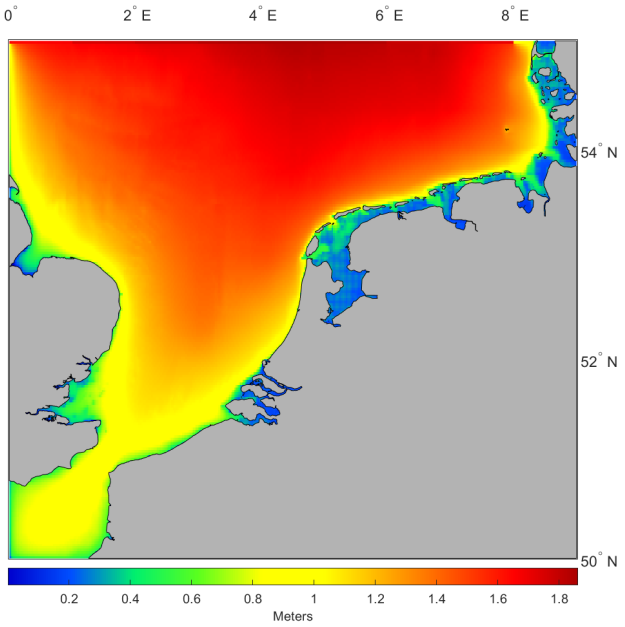

Fig. 9. Mean H_{m0} for 2015 from STH_{123}

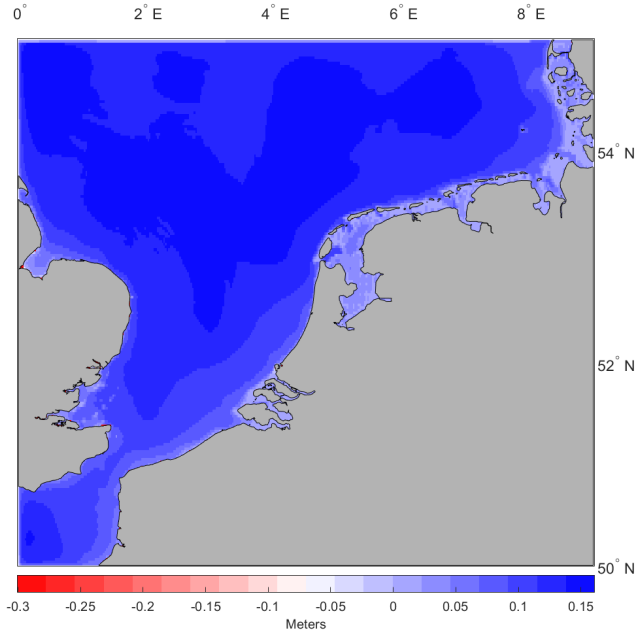

Fig. 10. H_{m0} differences in meters for STH_{123} versus the K_1

V. Discussion & Future work

The introduction of ST6 package in the SWAN model provides additional options in re-tuning wind drag coefficients, swell interaction and dissipation rates, therefore potential being more beneficial to mitigate the under-estimation of wave resource assessment.

From the calibration results we can see that the H_{m0} is obtains higher correlation than T_{m02}, as is expected wave models. The ST6 package allow the re-computation of stress and with the local and cumulative dissipation terms seems to reduce discrepancies. With using WAM 3 and WAM 4 the mean values were over and under-estimated respectively. With regards to H_{max} WAM 4 wind drag is hindcast with more "peaks" while WAM 3 consistently under-estimates.

ST6 offers a "middle" ground solution, when properly tuned. Tuning the dissipation ensures that wave frequencies are not often being turned from lower to higher, allowing a better computation of low frequency (high energy) waves. Within the ST6 package for our model of the North Sea we found that the most suitable configuration is based on adapting the Hwang wind drag coefficient, adopting dissipation terms according to option 2 and using utilizing the re-computation of dissipation terms to minimise under-estimations. The scaling option had little effect but indeed the higher option allowed for better maxima hindcast. Moreover, it is highly advised to activate the linear growth as we noticed more under-estimates in the performance.

Although, we cannot expect that numerical wave models will be explicitly deterministic in their assessment, a major improvement has been introduced with this configuration, when also compared with other wind drag and dissipation parametrisations it is observable that the bias is reduced but most importantly the highest waves are well "captured".

Future work includes building upon the calibrated model to produce a wave energy resource assessment for the Netherlands. Subsequent work will use the lessons learned by this study, and initiate a detail metocean characterisation for the region and validation of the model over multiple years with in-situ data.

ACKNOWLEDGEMENT

The authors would like to thank the anonymous reviewers for their constructive comments, that helped improve the manuscript.

REFERENCES

[1] L. Cavaleri, "Wave Modeling-Missing the Peaks," *Journal of Physical Oceanography*, vol. 39, no. 11, pp. 2757–2778, nov 2009. [Online]. Available: http://journals.ametsoc.org/doi/abs/10.1175/2009JPO4067.1

[2] J. E. Stopa and K. F. Cheung, "Intercomparison of wind and wave data from the ECMWF Reanalysis Interim and the NCEP Climate Forecast System Reanalysis," *Ocean Modelling*, vol. 75, pp. 65–83, mar 2014. [Online]. Available: http://linkinghub.elsevier.com/retrieve/pii/S1463500313002205

[3] G. Lavidas, V. Venugopal, and D. Friedrich, "Sensitivity of a numerical wave model on wind re-analysis datasets," *Dynamics of Atmospheres and Oceans*, vol. 77, pp. 1–16, 2017. [Online]. Available: http://linkinghub.elsevier.com/retrieve/pii/S0377026516301154

[4] E. B. Mackay, A. S. Bahaj, and P. G. Challenor, "Uncertainty in wave energy resource assessment. Part 1: Historic data," *Renewable Energy*, vol. 35, no. 8, pp. 1792–1808, 2010. [Online]. Available: http://dx.doi.org/10.1016/j.renene.2009.10.026

[5] D. Ingram, G. H. Smith, C. Ferriera, and H. Smith, "Protocols for the Equitable Assessment of Marine Energy Converters," Institute of Energy Systems, University of Edinburgh, School of Engineering, Tech. Rep., 2011. [Online]. Available: http://www.equimar.org/

[6] G. Lavidas and V. Venugopal, "Application of numerical wave models at European coastlines : A review," *Renewable and Sustainable Energy Reviews*, vol. 92, no. October 2016, pp. 489–500, 2018. [Online]. Available: https://doi.org/10.1016/j.rser.2018.04.112

[7] "Swan 41.20," Delft University of Technology Faculty of Civil Engineering and Geosciences Environmental Fluid Mechanics Section, 2018. [Online]. Available: http://swanmodel.sourceforge.net/

[8] D. P. Dee, S. M. Uppala, A. J. Simmons, P. Berrisford, P. Poli, S. Kobayashi, U. Andrae, M. A. Balmaseda, G. Balsamo, P. Bauer, P. Bechtold, A. C. M. Beljaars, L. van de Berg, J. Bidlot, N. Bormann, C. Delsol, R. Dragani, M. Fuentes, A. J. Geer, L. Haimberger, S. B. Healy, H. Hersbach, E. V. Holm, L. Isaksen, P. Kallberg, M. Kohler, M. Matricardi, A. P. Mcnally, B. M. Monge-Sanz, J. J. Morcrette, B. K. Park, C. Peubey, P. de Rosnay, C. Tavolato, J. N. Thepaut, and F. Vitart, "The ERA-Interim reanalysis: Configuration and performance of the data assimilation system," *Quarterly Journal of the Royal Meteorological Society*, vol. 137, no. 656, pp. 553–597, 2011.

[9] A. Akpinar, B. Bingölbali, and H. Jafali, "Wave Hindcasting for Wave Energy Assessments in the Black Sea," in *International Conference on Engineering and Natural Science (ICENS)*, Sarajevo, 2016, pp. 1–8.

[10] A. Agarwal, V. Venugopal, and G. P. Harrison, "The assessment of extreme wave analysis methods applied to potential marine energy sites using numerical model data," *Renewable and Sustainable Energy Reviews*, vol. 27, pp. 244–257, nov 2013. [Online]. Available: http://linkinghub.elsevier.com/retrieve/pii/S1364032113004401

[11] A. Akpinar and S. Ponce de León, "An assessment of the wind re-analyses in the modelling of an extreme sea state in the Black Sea," *Dynamics of Atmospheres and Oceans*, vol. 73, no. January 2016, pp. 61–75, 2016. [Online]. Available: http://linkinghub.elsevier.com/retrieve/pii/S0377026515300129

[12] L. Mentaschi, G. Besio, F. Cassola, and A. Mazzino, "Performance evaluation of Wavewatch III in the Mediterranean Sea," *Ocean Modelling*, 2015. [Online]. Available: http://linkinghub.elsevier.com/retrieve/pii/S1463500315000578

[13] ECMWF, "ERA Interim." [Online]. Available: http://www.ecmwf.int/

[14] C. Amante and B. Eakins, "ETOPO1 1 Arc-Minute Global Relief Model: Procedures, Data Sources and Analysis. NOAA Technical Memorandum NESDIS NGDC-24," 2014. [Online]. Available: http://maps.ngdc.noaa.gov/viewers/wcs-client/

[15] "Wavewatch3, manual v5.16." [Online]. Available: http://polar.ncep.noaa.gov/waves/wavewatch/manual.v5.16.pdf

[16] G. Komen, S. Hasselmann, and K. Hasselmann, "On the Existence of a Fully Developed Wind-Sea Spectrum.pdf," *Physical Oceanography*, vol. 14, pp. 1271–1285, 1984.

[17] P. A. Janssen, "Quasi-Linear theory of Wind-Wave Generation applied to wave forecasting," *Journal of Physical Oceanography*, vol. 6, pp. 1631–1642, 1991.

[18] A. J. van der Westhuysen, M. Zijlema, and J. Battjes, "Nonlinear saturation-based whitecapping dissipation in SWAN for deep and shallow water," *Coastal Engineering*, vol. 54, no. 2, pp. 151–170, feb 2007. [Online]. Available: http://linkinghub.elsevier.com/retrieve/pii/S037838390600127X

[19] S. Zieger, A. V. Babanin, W. Erick Rogers, and I. R. Young, "Observation-based source terms in the third-generation wave model WAVEWATCH," *Ocean Modelling*, 2015. [Online]. Available: http://linkinghub.elsevier.com/retrieve/pii/S1463500315001237

[20] P. A. Hwang, "A note on the ocean surface roughness spectrum," *Journal of Atmospheric and Oceanic Technology*, vol. 28, no. 3, pp. 436–443, 2011. [Online]. Available: https://doi.org/10.1175/2010JTECHO812.1

[21] Y. Fan, S.-J. Lin, I. M. Held, Z. Yu, and H. L. Tolman, "Global ocean surface wave simulation using a coupled atmosphere–wave model," *Journal of Climate*, vol. 25, no. 18, pp. 6233–6252, 2012. [Online]. Available: https://doi.org/10.1175/JCLI-D-11-00621.1

[22] F. Ardhuin, E. Rogers, A. V. Babanin, J.-F. Filipot, R. Magne, A. Roland, A. van der Westhuysen, P. Queffeulou, J.-M. Lefevre, L. Aouf, and F. Collard, "Semiempirical dissipation source functions for ocean waves. part i: Definition, calibration, and validation," *Journal of Physical Oceanography*, vol. 40, no. 9, pp. 1917–1941, 2010. [Online]. Available: https://doi.org/10.1175/2010JPO4324.1

[23] M. Zijlema, G. P. van Vledder, and L. Holthuijsen, "Bottom friction and wind drag for wave models," *Coastal Engineering*, vol. 65, pp. 19–26, jul 2012. [Online]. Available: http://linkinghub.elsevier.com/retrieve/pii/S0378383912000440

[24] W. E. Rogers, A. V. Babanin, and D. W. Wang, "Observation-consistent input and whitecapping dissipation in a model for wind-generated surface waves: Description and simple calculations," *Journal of Atmospheric and Oceanic Technology*, vol. 29, no. 9, pp. 1329–1346, 2012. [Online]. Available: https://doi.org/10.1175/JTECH-D-11-00092.1

[25] Rijkswaterstaat, "Open data rijkswaterstaat waterdienst,"

2018. [Online]. Available: https://www.rijkswaterstaat.nl/rws/opendata/